

# Green Synthesis of Cadmium Oxide Nanoparticles with Various Plant Extracts and their Use as an Anticancer Agent

Ashtosh Dixit <sup>1</sup>, Renu Bala <sup>1</sup>, Bhawna Pareek <sup>1,\*</sup>, Ashun Chaudhary <sup>2</sup>, Saroj Arora <sup>3</sup>, Davinder Singh <sup>3</sup>, Anju Bala <sup>4</sup>, Vivek Sheel Jaswal <sup>5,\*</sup>

<sup>1</sup> Department of Chemistry, Maharishi Markandeshwar (Deemed to be) University, Mullana, Ambala, Haryana; dixitashutosh376@gmail.com (A.D.); renusheoran031@gmail.com (R.B.); dr.pareekbhawna@gmail.com (B.P.);

<sup>2</sup> Department of Plant Science (Botany), Academic Block Shahpur, Central University of Himachal Pradesh, Dharamshala, Himachal Pradesh; ashunchaudhary@gmail.com (A.C.);

<sup>3</sup> Department of Botanical and Environmental Science, GuruNanak Dev University, Amritsar, Punjab; sarojarora.gndu@gmail.com (S.A.); sidhu.davinder0001@gmail.com (D.S.);

<sup>4</sup> Department of Physics, Maharishi Markandeshwar (Deemed to be) University, Mullana, Ambala, Haryana; anjukamboj134@gmail.com (A.B.);

<sup>5</sup> PG Department of Chemistry, SMDRSD College, Pathankot, Punjab; chemsheel@gmail.com (V.S.J.);

\* Correspondence: dr.pareekbhawna@gmail.com (B.P.); chemsheel@gmail.com (V.S.J.);

Scopus Author ID 22954445800

Received: 16.09.2021; Accepted: 14.10.2021; Published: 7.01.2022

**Abstract:** The co-precipitation method was used to produce cadmium oxide nanoparticles (CdO NPs) with different plant extracts such as *Tinospora Cardifolia* (stems), *Rhododendron arboretum* (flower), *Pichrorhiza Kurroa* (roots), *Nardostachys jatamansi* (roots), *Acorus Calamus* (roots), *Corylus Jacquemontii* (seeds), and *Emblica Officinalis* (fruit). To extract organic matter from the as-prepared sample, it was calcined at a temperature ranging from 500-600° C. X-ray diffraction (XRD), Scanning electron microscopy (SEM), Fourier transforms infrared spectroscopy (FTIR), and Transmission electron microscopy (TEM) were used to investigate the structure and morphology of the calcined oxide nanoparticles. The CdO NPs were well amorphous particle form and had an average particle size of 20-55 nm. The cytotoxicity of the *Pichrorhiza Kurroa* shows strong antiproliferative activity against rat skeletal myoblast cell lines (L-6).

**Keywords:** *Tinospora Cardifolia*; anticancer activity; FTIR; SEM; TEM; XRD.

© 2022 by the authors. This article is an open-access article distributed under the terms and conditions of the Creative Commons Attribution (CC BY) license (<https://creativecommons.org/licenses/by/4.0/>).

## 1. Introduction

Cadmium (Cd<sup>2+</sup>) is a rare genetically unregulated heavy metal, the most toxic to the living organism at relatively small levels and the most toxic environmental pollutant [1]. Different defense mechanism for overcoming Cd<sup>2+</sup> toxicity has been identified in a living organism [2]. Cadmium oxide (CdO) is an n-type semiconducting material used as a transparent conducting film preparation. Nanomaterials are used to produce highly-developed structural ceramics as oxides and starting materials [3]. CdO has potential uses in photovoltaic cells [4], detectors [5], catalysts [6], and solar cells [7], etc., as a versatile semiconductor. Cadmium oxide is used for a transparent electrode, phototransistor, fluid crystal panels, photodiode, and IR. The design of quick, easy, and cost-efficient procedures to synthesize nanoparticles in the field of nanotechnology is worthwhile. Therefore the synthesisation of these nanoparticles of different shapes and sizes is very important [8]. These factors had a

serious influence on and potential application of the physical and chemical properties of the sensing [9], optoelectronic [10], bimolecular detection [11], media recording [12], and medical devices [13]. The application of environmentally good materials such as leaves and flowers for nanoparticles synthesis and bacteria and fungi provides numerous pharmaceutical and biomedical safety benefits because no toxic chemicals are used in the synthesis protocols [14]. The existing literature discusses two basic principles of synthesis (i.e., top-down and bottom-up) to obtain nanomaterials of desirable sizes, compatibility, and shapes. Divergent synthesized methods such as lithography techniques, ball milling, and sputtering using nanomaterials/nanoparticles [15]. Besides, implementing a bottom-up method includes numerous techniques, including chemical vapor deposition, laser pyrolysis, and atomic/molecular condensation. Scientists have become aware of the use of cadmium oxides in optoelectric appliances in recent years, including sol-glassy electrodes, optical transistors, gas detectors, etc. [16]. The sonochemical synthesis is particularly attractive among various approaches to producing nanoparticles because of its performance, excellent returns, simplicity, and pure product quality [17].

The synthesis of nanoparticles from group 12 semiconductors (e.g., CdO, CdS, ZnO, and ZnS) is particularly interesting because of their volume, optical properties, electronic, and shape [18]. Also, a broad bandgap is a significant semiconductor of inorganic cadmium oxide [19]. Green synthesis has been introduced to store several biological materials in metallic nanoparticles. Bio-precursor-based green synthesis methodologies are dependent on various reaction parameters, such as temperature, solvent, pressure, and pH. The basic features for clinical diagnostics, catalysts, optical imaging, molecular scanning, antimicrobials, and biologic device labeling have been examined [20]. Cadmium oxide is a special chemical with semi-conductive and piezoelectric properties. The frequency of Exciton's binding energy (75meV) [21] and gap energy of about 4.05 (eV) is higher in comparison with other semiconductors [22-24]. Cadmium oxide (CdO) film was made using a range of techniques, e.g. magnetron sputtering [25,26], ball milling [27], deposition method [28] and sol-gel method [29-31]. Nanoparticles of cadmium oxide (CdO) are anticancer. Cadmium oxide (CdO) nanoparticles are important to scientists and researchers because of their peculiar optical, chemical, photo-electrochemical, and electrical properties [32]. DNA and protein damages and degradation of the cell wall are the key mechanism of cadmium oxide (CdO), which affects nanoparticles in cancer cells.

Interestingly, nanoparticles containing cadmium oxide (CdO) are not toxic to human and mammalian cells [33-37]. It is also used in cancer cell delivery of medicines. Each nanoparticle can carry only small amounts of cadmium oxide medicines with very small sizes [38-40]. Nanoparticles of cadmium oxide (CdO) have provided a new perspective to cancer prevention scientists and researchers. In different forms, nanoparticles made of cadmium oxide (CdO) are very much involved in pharmaceutical and medicinal research and, in particular, in research into applications of cancer treatment [41-43]. In this paper, Cadmium oxide nanoparticles are studying their effect on the DNA of cancer cells in humans and the interaction of the CdO nanoparticles with the DNA of cancer cells.

*Tinospora Cardifolia* is a dioecious plant belonging to the Menispermaceae family. It has been identified as anti-diabetic, anti-inflammatory, anti-oxidant, anti-malarial, and anti-stress [44]. *Rhododendron arboretum* is a well-known horticulture plant that has become one of the most common plants in gardens and avenue trees. It is widely cultivated in various parts of the world due to its ethnical and economics and medicinal values. People in the mountainous

area have historically used the flowers of this plant to make pickles, syrup, jelly, and other products and treat a variety of ailments such as diarrhea, headaches, and fungal infections [45]. *Pichrorhiza Kurroa* royal ex Benth (Family: Scrophulariaceae) is a medicinal plant that grows primarily in the North-Western Himalayas. *P. Kurroa* is a well-known Ayurveda herb that has been used to treat liver and upper respiratory tract disorders, reduce fevers and treat dyspepsia and chronic diarrhea [46]. *Nardostachys jatamansi* oil has been used as incense, a perfume, a sedative, and a natural remedy to treat insomnia and other minor ailments. *N. jatamansi* is a small, rough plant in the Valerianaceae family. The plant is sedative, antidepressant, hypertensive anti-inflammatory, and cardiotoxic in conventional medical systems [47]. *Acorus Calamus* is a natural plant that belongs to the Acoralus order and the Acoraceae family. This plant has a long history of medicinal use in Chinese and Indian herbal traditions, where it was used to treat dyspepsia, mouth and throat diseases, fever, tumors, earworms, chest and kidney pains, insomnia, asthma, and diarrhea [48]. *Corylus Jacquemontii* is a high-value multipurpose tree that is both ecologically and economically valuable in the Indian Himalayan region. Plant phytochemical constituents such as phenolic, flavonoids, terpenoids, tannins, and saponins are responsible for anti-inflammatory, antifungal, and anti-diabetic properties [49]. The fruit of the *Emblica Officinalis* (Amla) tree is commonly used in Ayurveda and is thought to improve disease resistance. It is useful in treating cancer, diabetes, liver disease, anemia, and various other diseases. It also has anti-oxidant, antitussive, cytoprotective, and antipyretic properties [50]. Plant extracts have medicinal potential as reducing and capping agents in the synthesis of NPs due to the presence of various phytochemicals such as alkaloids, terpenoids, vitamins, and phenols (8.62-54.6 mg CE/g).

## 2. Materials and Methods

All chemicals used in the experiment are analytic reagent grade. Cadmium sulfate [ $\text{CdSO}_4 \cdot \text{H}_2\text{O}$ ] was purchased from Merck, India. Ammonium hydroxide (liquor ammonia) was purchased from SRL. Deionized water was used throughout the experiment.

### 2.1. Synthesis of Cadmium oxide nanoparticles.

Deionized water was used to make a cadmium sulfate solution. *Tinospora Cardifolia* (stems), *Rhododendron arboretum* (flower), *Pichrorhiza Kurroa* (roots), *Nardostachys jatamansi* (roots), *Acorus Calamus* (roots), *Corylus Jacquemontii* (seeds), and *Emblica Officinalis* (fruit) were all used at 1% in 0.2 M cadmium sulfate using 200 ml Deionized water. 1% of the plant extract should be added to this solution. The extracts were combined, and aqueous ammonia was applied dropwise to the solution mixture while constantly stirring until the pH reached 10. For 3 hours, the mixture was stirred. The resulting precipitates were filtered through a Buckner funnel and washed with distilled water several times. The precipitates were dried in an oven for 24 hours before being calcined to remove any contamination in a muffle furnace at 600° C for 5 hours.

### 2.2. Preparation of the plant extract.

*Tinospora Cardifolia* (stems), *Rhododendron arboretum* (flower), *Pichrorhiza Kurroa* (roots), *Nardostachys jatamansi* (roots), *Acorus Calamus* (roots), *Corylus Jacquemontii* (seeds), and *Emblica Officinalis* (fruit) was thoroughly washed and dried completely in the shade. Dried (flower, stems, seeds, roots, fruit) are cut into small pieces and powdered in a

grinder. 100 grams of powder was mixed in ethanol and distilled water in a ratio of 1:1 and was heated for about 3 hours at 100° C. After cooling, and the extract was filtrated using Whatman No.1 filter paper. Collect filtrate and evaporate the solvent in a Rotary evaporator. We used dried leaves because it has a long-lasting effect, maintain cell structure and shape.

### 2.3. Characterization techniques.

Several techniques were used to characterize the NPs, including Fourier transform infrared spectroscopy (Perkin Elmer-spectrum RX-FTIR) in the 400 cm<sup>-1</sup> to 4000 cm<sup>-1</sup> range to study the functional group and chemical structure. Transmission electron microscopy was used to examine the morphology of CdO NPs. A drop of NPs was dropped onto a carbon-coated copper grid and allowed to dry at room temperature. A Hitachi (H-7500) with a 120 kV accelerating voltage and energy-dispersive X-ray spectroscopy (EDS) was used for TEM micrographs, and the same instrument was used for elemental mapping. Image J software was used to perform TEM diameter measurements. Panalytical's Xpert Pro measured X-ray diffraction of CdO NPs. The crystalline and morphology of CdO NPs were studied at a temperature ranging from 10-80° C. scanning electron microscope model JSM6100 was used to examine the form and size of NPs (Jeol).

### 2.4. Anticancer activity.

#### 2.4.1. Cell lines and culture.

In a tissue culture flask, immortalized rat skeletal myoblast cells (L-6) were cultured and preserved in DMEM medium (HiMedia) supplemented with 10% FBS (fetal bovine serum) and antibiotics (100 U/ml penicillin, 100gm/ml streptomycin) in a CO<sub>2</sub> incubator at 37° C, 5% CO<sub>2</sub>, and 95% relative humidity. Cells were harvested at the log step of growth for different analyses, and the medium was modified regularly. Untreated control cultures received only DMSO, while extracts dissolved in DMSO were used to treat the cells.

#### 2.4.2. MTT assay.

The protocol was used to study the cytotoxicity potential of bioinspired CdO NPs *in vitro* against the cancer cell line L6 and cells were cultured in supplemented DMEM media. The cells were grown at 37° C in the incubator with 5% CO<sub>2</sub>. The MTT assay was performed in 96 well microplates at different concentrations by incubating for 48h, and 20 µL of MTT were added to each well and maintained in an incubator for 3h. The media was discarded, and 100 µL of DMSO was added for 3 min. The number of viable and nonviable cells was monitored in a spectrophotometer at a wavelength of 517 nm.

#### 2.4.3. MMP process.

MMP assay had been performed by protocol Deng *et al.*, 2013. In this protocol, the cancer cells are removed from culture flasks with trypsin and determine their viability with trypan blue dye. The required 96 well-plates at the density of 1\*10<sup>5</sup>- 3\*10<sup>5</sup> cells/well in 1ml/well growth medium have been added in this type of cancer cell. The plate was incubated (5% CO<sub>2</sub>& 37°C) for 24 hrs and the medium was discarded. after IC<sub>50</sub> and IC<sub>70</sub> of compounds prepared in growth media have been added and incubated for 24 hrs after incubation, each medium was discarded, and the newly prepared dye has been applied (10µg rhodamine, 123

dye/ml of FBS growth medium) to each well (1ml/well). The medium was carefully discharged, and the cells were washed using 1\* sterile PBS, which added 1ml of fresh PBS in each well and measured with a 485nm excitation microplate reader and 528nm emission.

#### 2.4.4. ROS process.

The cells in 96 well plates were allowed to settle down and adhere for 6 hrs and then cultured with or without extract for 24 hrs. The cells were caught by collecting medium and trypsin cells from floating cells after 12 hrs of treatment. The 2, 7- dichlorofluorescein diacetate (DCFHDA) was added after treatment was over. The cell pellet was centrifuged and solubilized into cold PBS (100µl). The DCFHDA has been used to determine L-6 cells treated with extract for 12 hrs at respective IC<sub>50</sub>. The cell was analyzed at 485nm (Excitation); and 528(Emission).

### 3. Results and Discussion

#### 3.1. XRD.

Diffraction peaks were absorbed in 2θ values 20.2°, 23.4°, 30.3°, 51.1°, 55.6°, 68.7°, and 70.6°, respectively in the XRD patterns of the CdO nanostructure shown in figure 1. The Scherrer equation (1) was used to measure the grain size using the prominent peaks

$$D = \frac{\kappa\lambda}{\beta} \cos\theta \quad \text{Eq (1) [51]}$$

where λ is the wavelength, β is the full width at half the maximum of the line, and θ is the diffraction angle.

According to Stevenson *et al.* [52], the diffraction pattern was also consistent with the hexagonal CdO process. The reflection (111), (200), (220), and (311) are visible and closely match the CdO reference pattern. This confirms the formation of CdO NPs as verified by JCPDF Card NO.: 65-2908. The polycrystalline nature of the particles and the random orientation of the nanostructure are shown by the sharp XRD peaks [53]. The average size of the CdO nanoparticles was found to be in the 20-55 nm range.

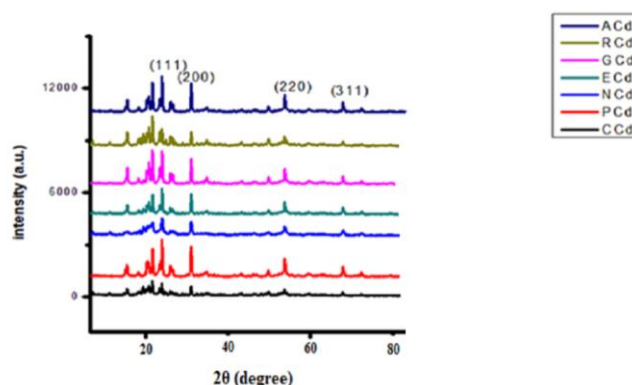


**Figure 1.** XRD patterns of CdO NPs with different plants extract.

#### 3.2. SEM.

Cadmium ions are reduced at room temperature, resulting in the formation of nanoparticles. The SEM analysis of the structure of CdO nanoparticles and their morphological dimensions revealed that the average particle size was 20-55 nm. The shape was amorphous,

shown in figure 2. The image depicts CdO nanoparticles generated by *Tinospora Cardifolia* (stems), *Rhododendron arboretum* (flower), *Pichrorhiza Kurroa* (roots), *Nardostachys jatamansi* (roots), *Acorus Calamus* (roots), *Corylus Jacquemontii* (seeds), and *Emblica Officinalis* (fruit) extracts.

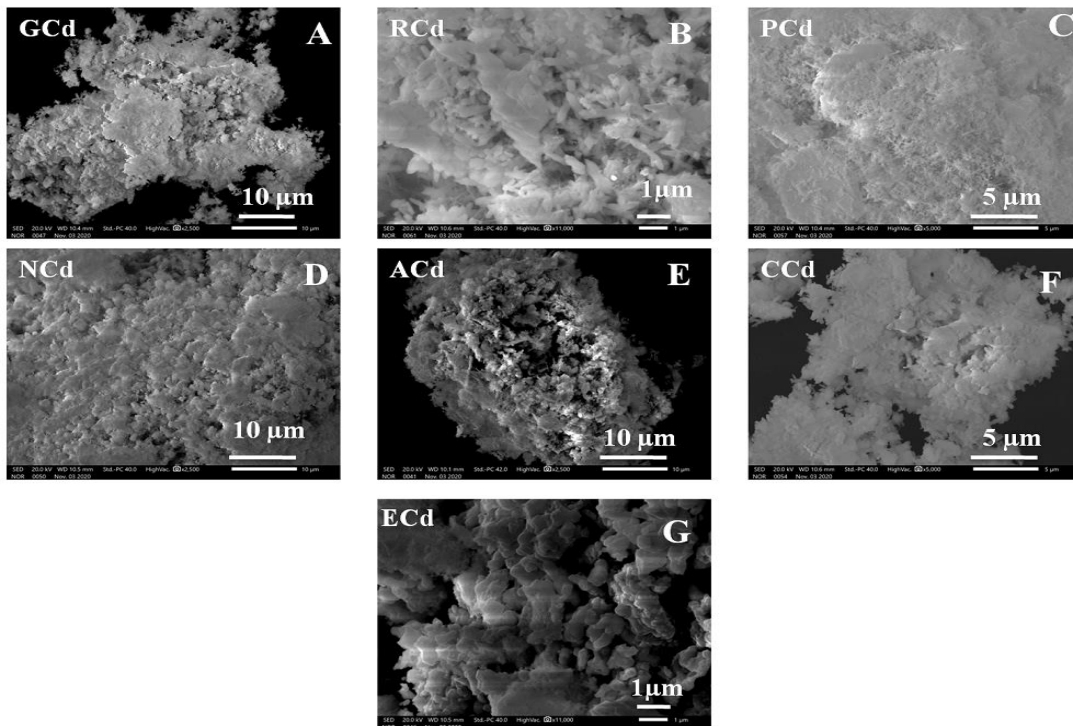


**Figure 2.** SEM images of the synthesized CdO NPs with different plant extracts.

### 3.3. TEM.

The particle size distribution was shown in figure 3 in the TEM picture of the CdO nanoparticles corresponding to the same sample of XRD pattern in figure 1 and SEM in figure 2.

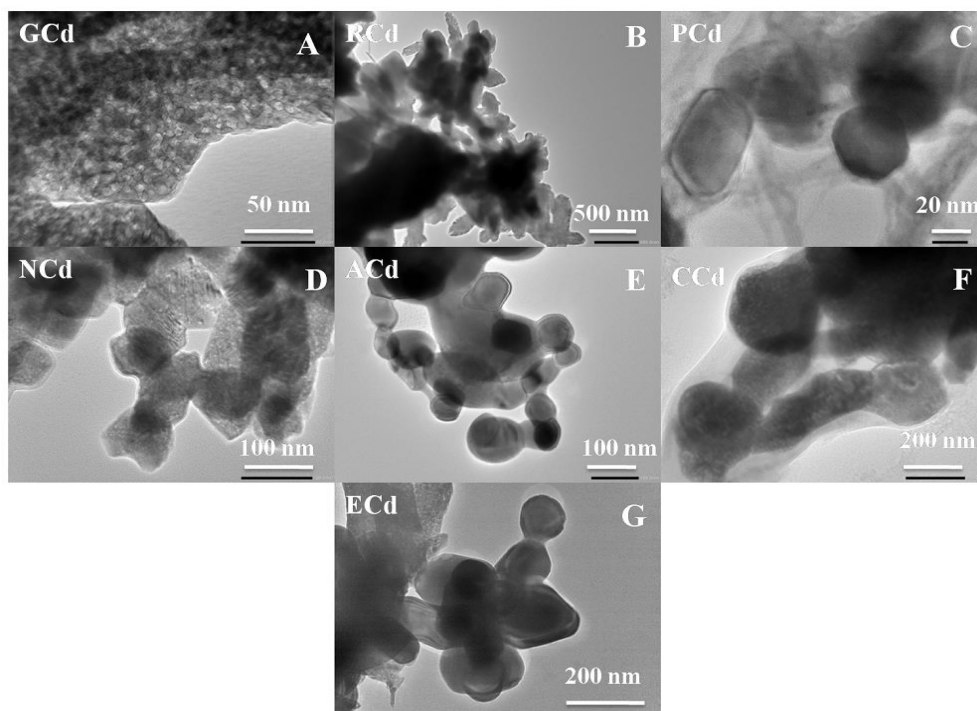


**Figure 3.** TEM images of various CdO NPs with different plant extracts.

According to TEM, the average particle size tends to be about 20-55nm. The high-resolution electron microscope image showed that these particles are single crystalline. The particles have an amorphous form, similar to Dong *et al.* [54]. Image J software was also used to identify the particle size by the histogram, as shown in figure 4. The histogram of the CdO NPs particle size distribution is sizes range from 42.41±2.3, 53±1.5, 31.38±1.6, 51.63±2.2, 40.85±2.2, 41.2±2.4, and 50.14±2.8 nm, respectively.

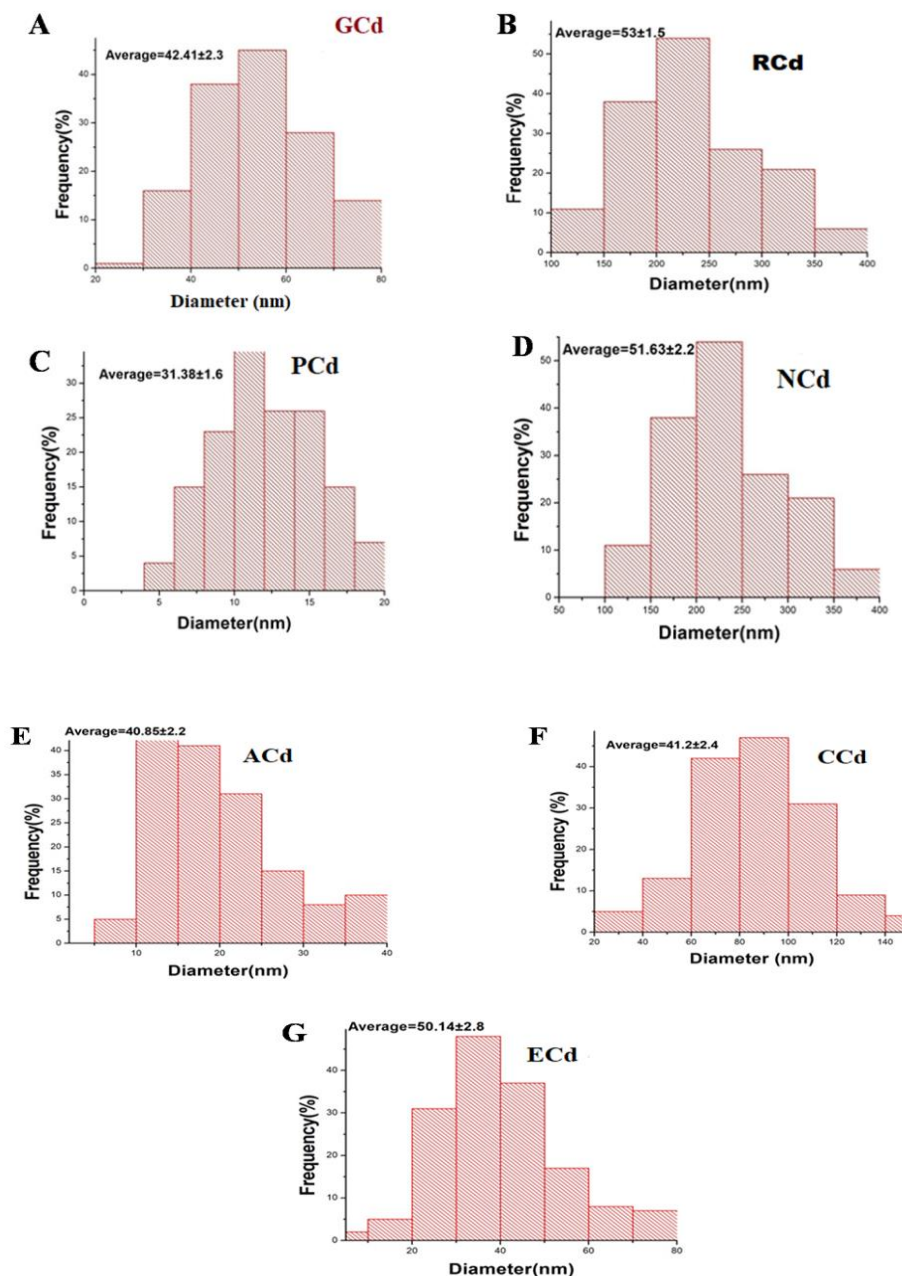


**Figure 4.** Histogram images of synthesized CdO NPs.

### 3.4. FT-IR.

FTIR identified the biomolecules responsible for the reduction of Cd ions and capping of reduced CdO nanoparticles synthesized by the *Tinospora Cardifolia* (stems), *Rhododendron arboretum* (flower), *Pichrorhiza Kurroa* (roots), *Nardostachys jatamansi* (roots), *Acorus Calamus* (roots), *Corylus Jacquemontii* (seeds) and *Emblca Officinalis* (fruit) extracts. Figure 5 shows that *Tinospora Cardifolia* (GCd) peaks at 2355 (C-C stretching), 2087 (primary

amines), 1051 (C-O stretching), *Rhododendron arboretum* (RCd) peaks at 2318 (C-C stretching), 2087 (primary amines), 1058 (C-O stretching), *Pichrorhiza Kurroa* (PCd) peaks at 2087 (primary amines), 1058 (C-O stretching), *Nardostachys jatamansi* (NCd) peaks at 2318 (C-C stretching), 2087 (primary amines), 1051 (C-O stretching) and figure 6 show *Acorus Calamus* (ACd) peaks at 2094 (primary amines), 1058 (C-O stretching), *Corylus Jacquemontii* (CCd) peaks at 2974 (C-H stretching), 2087 (primary amines), 2363 (C-C stretching), 1058 (C-O stretching) and *Embllica Officinalis* (ECd) peaks at 3481 (O-H stretching), 2087 (primary amines), 1103 (-OCH<sub>3</sub>). The Cd-O (metal-oxygen) vibration is correlated with the FTIR peaks at 450-650 cm<sup>-1</sup>. The difference in peak positions suggested that certain metabolites such as tannins, alkaloids, and flavonoids are abundant in lower extract and produce CdO nanoparticles.

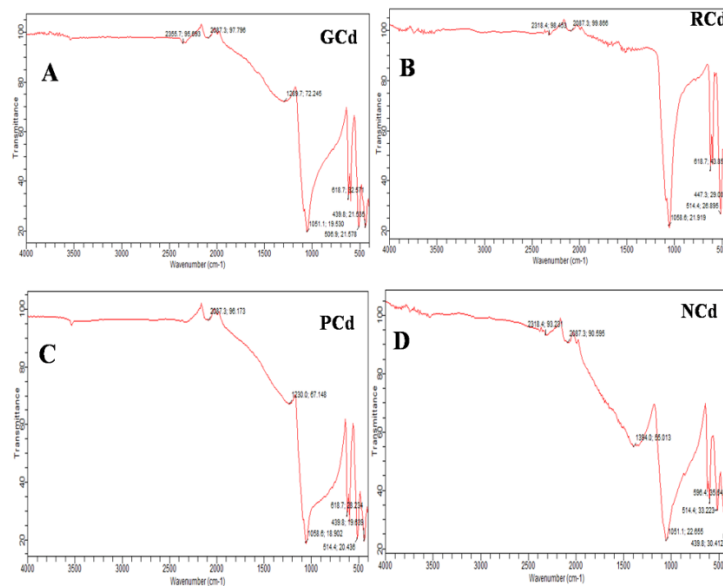


**Figure 5.** FTIR structure of different plant extracts of CdO NPs.

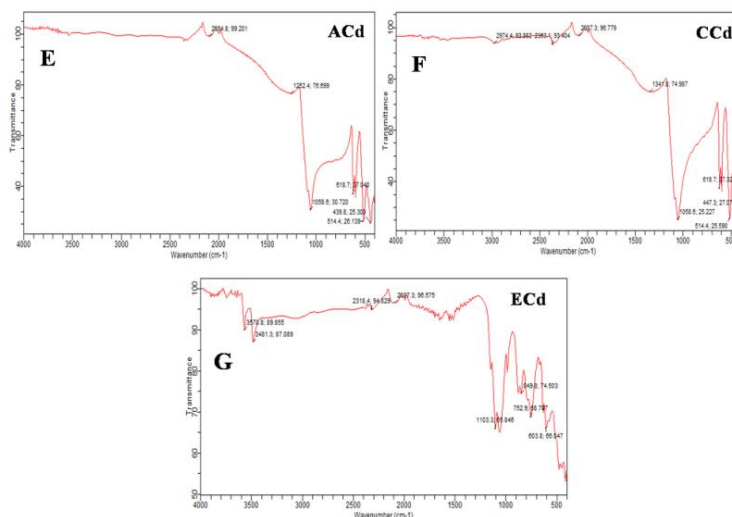


**Figure 6.** FTIR structure of different plant extracts of CdO NPs.

### 3.5. Anticancer activity.

#### 3.5.1. MTT assay analysis.

*Pichrorhiza Kurroa* (PCd) was the only one of the seven compounds that had a significant antiproliferative effect on immortalized rat skeletal myoblast cells. The IC<sub>50</sub> was

determined to be 0.0927 mg/ml. At concentrations of 0.0937 and 0.0929 mg/ml, CCd and NCd displayed antiproliferative activity, respectively inhibiting 50% of cells. GCd, RCd, PCd, NCd, ACd, CCd, and ECd were the NPs that displayed the most operation in figure 7.

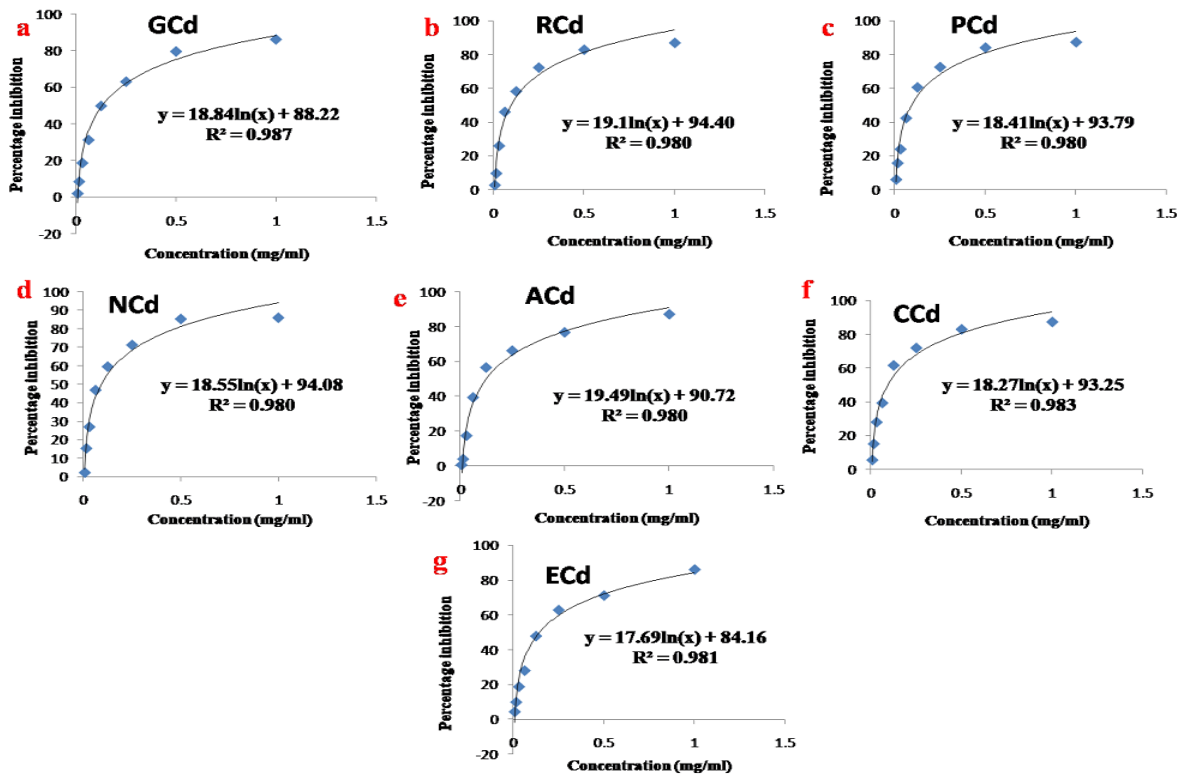


**Figure 7.** Different plants have different effects on MTT production in L6 cells.

### 3.5.2. ROS assay analysis.

The mechanism of cellular death was investigated using a test for reactive oxygen species. DCFHDA is a non-fluorescent molecule that can freely move about inside cells. Cellular esterase transforms it to DCFH, a non-fluorescent compound. Reactive oxygen species oxidize DCFH to DCF, a highly fluorescent compound. The compound Pichrorhiza Kurroa (PCd) increased the most ROS concentration, followed by GCd, RCd, NCd, ACd, CCd, and ECd shown in figure 8. PCd IC<sub>50</sub> concentration produces a 1.14 fold rise in ROS levels in cells. The developed ROS was increased to 1.28 after treatment with IC<sub>70</sub> concentrations.

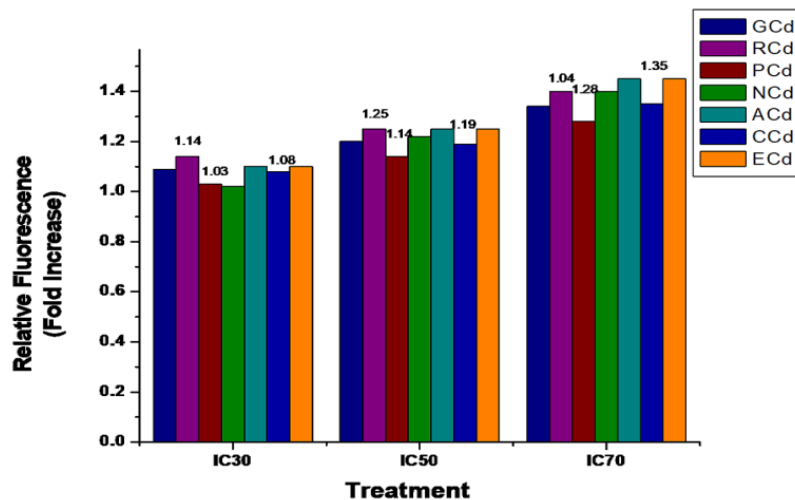


**Figure 8.** The effect of different plants on the production of reactive oxygen species (ROS) in L6 cells.

### 3.5.3. MMP assay analysis.

The reactive oxygen species formed by the compounds decreased the mitochondrial membrane ability (MMP). Apoptotic factors leak into the cytosol as a result, including apoptosis. Of the seven compounds, *Pichrorhiza Kurroa* (PCd) has the best activity against L-6 cells that are highly proliferative, shown in figure 9. Treatment with IC<sub>50</sub> concentration of PCd causes a reduction in MMP, as measured by a drop in rhodamine strength from 100% to 57.8%, with IC<sub>70</sub> concentration causing a further drop to 54.21%.

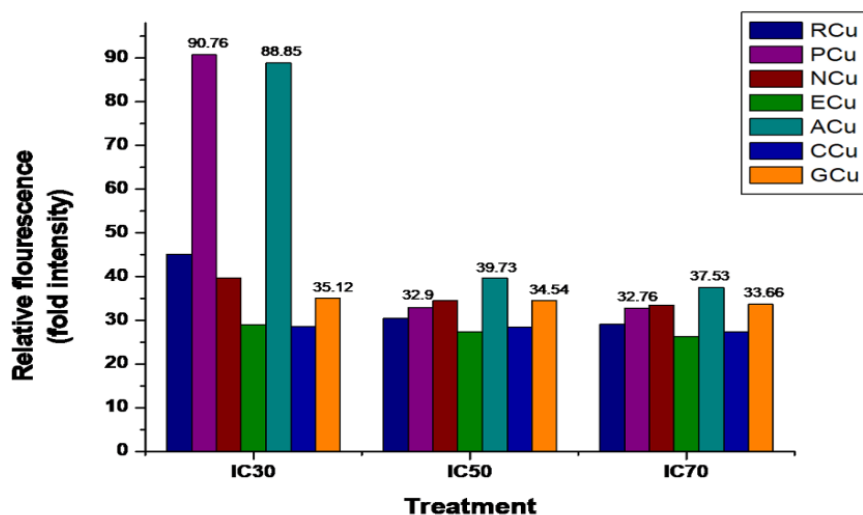


**Figure 9.** The effect of various plants on the production of mitochondrial membrane potential (MMP) in L6 cells.

## 4. Conclusions

In conclusion, different plant extracts such as *Tinospora Cardifolia* (stems), *Rhododendron arboretum* (flower), *Pichrorhiza Kurroa* (roots), *Nardostachys jatamansi* (roots), *Acorus Calamus* (roots), *Corylus Jacquemontii* (seeds), and *Embllica Officinalis* (fruit) were used to achieve green and rapid biosynthesis of CdO NPs. Plant extracts that include alkaloids, flavonoids, and other functional groups are assumed to be responsible for forming Cadmium oxide nanoparticles. The CdO NPs were synthesized and examined by using FT-IR, XRD, TEM, and SEM. According to TEM research, plant extract concentration has a limited effect on the size of CuO NPs. After microscopic SEM & TEM study reveals, the CdO NPs were discovered to be amorphous in shape with a size of 20-55 nm. To study the cytotoxicity of NPs we used the L-6 rat skeleton cell line. CdO NPs decreased cell viability in the L-6 cell line according to MTT assay. According to inverted microscopy results, *Pichrorhiza Kurroa* has the most cytotoxic effect on L-6 cells, with an IC<sub>50</sub> of 0.0927 mg/ml. The application of different extracts with ROS and MMP resulted in an IC<sub>50</sub> of 1.14 and 57.8%, respectively.

## Funding

This research received no external funding.

## Acknowledgments

This research was supported by Maharishi Markandeshwar (Deemed to be) University, Guru Nanak Dev University Amritsar, and SMDRSD college Pathankot, Punjab.

## Conflicts of Interest

The authors declare no conflict of interest.

## References

1. Stankovic, S.; Stankovic, A.R. Bioindicators of toxic metals. In: *Green materials for energy, products, and depollution*. Springer, Dordrecht. **2013**; 151-228, [https://doi.org/10.1007/978-94-007-6836-9\\_5](https://doi.org/10.1007/978-94-007-6836-9_5).
2. Al-Ragehey, A.S.; Dakhil, O.A.A.; Saadoun, H.; Mohammed, A.H.; Hassan, M. Employment of DC Sputtering for Synthesizing Nano Cadmium Oxide for Sevoflurane Anesthetic Gas Sensor. *Materials Science Forum*. **2021**, *1039*, 406-415, <https://doi.org/10.4028/www.scientific.net/MSF.1039.406>.
3. Reddy, K.C.S.; Kumar, K.S.; Yadav, L.R. Synthesis and characterization of magnesium oxide nanoparticles using combustion method to study the fuel properties. *Materials Today: Proceedings* **2021**, <https://doi.org/10.1016/j.matpr.2021.05.297>.
4. Kumari, R.; Kumar, V. Impact of zinc doping on structural, optical, and electrical properties of CdO film prepared by sol-gel screen printing mechanism. *Journal of Sol-Gel Science and Technology* **2020**, *94*, 648-657, <https://doi.org/10.1007/s10971-019-05202-0>.
5. Ye, C.; Xu, F.; Wu, Z.; Gao, Z.F.; Wang, M. Ultra sensitive photo electrochemical platform with micro-emulsion-based p-type hollow silver iodide enabled by low solubility product (K<sub>sp</sub>) for H<sub>2</sub>S sensing. *Nanotechnology* **2021**, *32*, <https://doi.org/10.1088/1361-6528/ac1094>.
6. Shashanka, R.; Jayaprakash, G.K.; Kumar, M.; Kumara Swamy, B.E. Electro catalytic determination of ascorbic acid using a green synthesised magnetite nano-flake modified carbon paste electrode by cyclic voltametric method. *Materials Research Innovations* **2021**, 1-11, <https://doi.org/10.1080/14328917.2021.1945795>.
7. Shashanka, R. Investigation of optical and thermal properties of CuO and ZnO nanoparticles prepared by Crocus Sativus (Saffron) flower extract. *Journal of the Iranian Chemical Society* **2021**, *18*, 415-427, <https://doi.org/10.1007/s13738-020-02037-3>.
8. Mukherjee, P.; Ahmad, A.; Mandal, D.; Senapati, S.; Sainkar, S.R.; Khan, M.I.; Sastry, M. Fungus-mediated synthesis of silver nanoparticles and the immobilization in the mycelial matrix: a novel biological approach to nanoparticle synthesis. *Nanoletters*. **2001**, *1*, 515-519, <https://doi.org/10.1021/nl0155274>.
9. Han, M.; Gao, X.; Su, J.Z.; Nie, S. Quantum-dot-tagged microbeads for multiplexed optical coding of biomolecules. *Nature biotechnology* **2001**, *19*, 631-635, <https://doi.org/10.1038/90228>.
10. Jin, R.; Cao, Y.; Mirkin, C.A.; Kelly, K.L.; Schatz, G.C.; Zheng, J.G. Photoinduced conversion of silver nanospheres to nanoprisms. *Science*. **2001**, *294*, 1901-1903, <https://doi.org/10.1126/science.1066541>.
11. Rosi, N.L.; Mirkin, C.A. Nanostructures in biodiagnostics. *Chemical reviews* **2005**, *105*, 1547-1562, <https://doi.org/10.1021/cr030067f>.
12. He, J.; Wu, C.; Li, Y.; Li, C. Design of pre-catalysts for heterogeneous CO<sub>2</sub> electrochemical reduction. *Journal of Materials Chemistry A* **2021**, *9*, 19508-19533, <https://doi.org/10.1039/D1TA03624F>.
13. Sonkar, R.; Jha, A.; Viswanadh, M.K.; Burande, A.S.; Pawde, D.M.; Patel, K.K.; Muthu, M.S. Gold liposomes for brain-targeted drug delivery: Formulation and brain distribution kinetics. *Materials Science and Engineering: C* **2021**, *120*, <https://doi.org/10.1016/j.msec.2020.111652>.
14. Mohanpuria, P.; Rana, N.K.; Yadav, S.K. Biosynthesis of nanoparticles: technological concepts and future applications. *Journal of nanoparticle research*. **2008**, *10*, 507-517, <https://doi.org/10.1007/s11051-007-9275-x>.
15. Cao, G. *Nanostructures & nanomaterials: synthesis, properties & applications*. Imperial college press. **2004**.
16. Sujatha, K.; Sharmila, S.; Sudha, A.P.; Shanmuga sundaram, O.L. Surfactant assisted spectroscopic application of cadmium oxide nanoparticles prepared via co-precipitation method. *Materials Today: Proceedings* **2021**, <https://doi.org/10.1016/j.matpr.2021.03.626>.
17. Chatel, G.; Colmenares, J.C. Sonochemistry: from Basic Principles to Innovative Applications. *Topics in Current Chemistry* **2017**, *375*, <https://doi.org/10.1007/s41061-016-0096-1>.
18. Fernandez-Garcia, M.; Martinez-Arias, A.; Hanson, J.C.; Rodriguez, J.A. Nano structured oxide thin chemistry: characterization and properties. *Chemical reviews* **2004**, *104*, 4063-4104, <https://doi.org/10.1021/cr030032f>.
19. Jefferson, P.H.; Hatfield, S.A.; Veal, T.D.; King, P.D.C.; McConville, C.F.; Zúñiga-Pérez, J.; Muñoz-Sanjosé, V. Band gap and effective mass of epitaxial cadmium oxide. *Applied Physics Letters* **2008**, *92*, <https://doi.org/10.1063/1.2833269>.
20. Aguilar, Z. *Nanomaterials for medical applications*. Newnes. **2012**.
21. Shashanka, R.; Esgin, H.; Yilmaz, V.M.; Caglar, Y. Fabrication and characterization of green synthesized ZnO nanoparticle based dye-sensitized solar cells. *Journal of Science: Advanced Materials and Devices* **2020**, *5*, 185-191, <https://doi.org/10.1016/j.jsamd.2020.04.005>.
22. Sharma, M.K.; Narayanan, J.; Upadhyay, S.; Goel, A.K. Electrochemical immuno sensor based on bismuth nano composite film and cadmium ions functionalized titanium phosphates for the detection of anthrax

- protective antigen toxin. *Biosensors and Bioelectronics* **2015**, *74*, 299-304, <https://doi.org/10.1016/j.bios.2015.06.015>.
23. Gupta, V.K.; Pathania, D.; Asif, M.; Sharma, G. Liquid phase synthesis of pectin–cadmium sulfide nano composite and its photocatalytic and antibacterial activity. *Journal of Molecular Liquids* **2014**, *196*, 107-112, <https://doi.org/10.1016/j.molliq.2014.03.021>.
24. Wang, W.S.; Zhen, L.; Shao, W.Z.; Chen, Z.L. Sodium chloride induced formation of square-shaped cadmium molybdate nanoplates. *Materials Letters*. **2014**, *131*, 292-294, <https://doi.org/10.1016/j.matlet.2014.05.203>.
25. Mahmoud, K.H.; El-Bahy, Z.M.; Hanafy, A.I. Photo luminescence analysis of Er nanoparticles in cadmium-phosphate glasses. *Journal of non-crystalline solids* **2013**, *363*, 116-120, <https://doi.org/10.1016/j.jnoncrsol.2012.12.004>.
26. Sharma, R.K.; Kedarnath, G.; Wadawale, A.; Jain, V.K.; Vishwanadh, B. Monomeric pyridyl-2-selenolate complexes of cadmium and mercury: Synthesis, characterization and their conversion to metal selenide nanoparticles. *Inorganica Chimica Acta* **2011**, *365*, 333-339, <https://doi.org/10.1016/j.ica.2010.09.039>.
27. Rajendrachari, S.; Kamacı, Y.; Taş, R.; Ceylan, Y.; Bülbül, A.S.; Uzun, O.; Karaođlanlı, A.C. Antimicrobial investigation of CuO and ZnO nanoparticles prepared by a rapid combustion method. *Physical Chemistry Research* **2019**, *7*, 799-812, <https://doi.org/10.22036/pcr.2019.199338.1669>.
28. Rajendrachari, S.; Yilmaz, V.M.; Karaoglanli, A.C.; Uzun, O. Investigation of activation energy and antibacterial activity of CuO nano-rods prepared by Tilia Tomentosa (Ihlamur) leaves. *Moroccan Journal of Chemistry* **2020**, *8*, <https://doi.org/10.48317/IMIST.PRSM/morjchem-v8i2.17765>.
29. Mthethwa, T.; Pullabhotla, V.R.; Mdluli, P.S.; Wesley-Smith, J.; Revaprasadu, N. Synthesis of hexa decylamine capped CdS nanoparticles using heterocyclic cadmium dithio carbamates as single source precursors. *Polyhedron*. **2009**, *28*, 2977-2982, <https://doi.org/10.1016/j.poly.2009.07.019>.
30. Rajendrachari, S.; Kumara swamy, B.E. Biosynthesis of silver nanoparticles using leaves of Acacia melanoxylon and their application as dopamine and hydrogen peroxide sensors. *Physical Chemistry Research* **2020**, *8*, 1-18, <https://doi.org/10.22036/pcr.2019.205211.1688>.
31. Thornton, J.M.; Raftery, D. Hydrogen evolution by templated cadmium in date nanoparticles under natural sunlight illumination. *International journal of hydrogen energy* **2013**, *38*, 7741-7749, <https://doi.org/10.1016/j.ijhydene.2013.04.039>.
32. Rajendrachari, S.; Karaoglanli, A.C.; Ceylan, Y.; Uzun, O.A. Fast and Robust Approach for the Green Synthesis of Spherical Magnetite (Fe<sub>3</sub>O<sub>4</sub>) Nanoparticles by Tiliatomentosa (Ihlamur) Leaves and its Antibacterial Studies. *Pharmaceutical Sciences* **2020**, *26*, 175-183, <https://doi.org/10.34172/PS.2020.5>.
33. Malekigorji, M.; Curtis, A.D.; Hoskins, C. The use of iron oxide nanoparticles for pancreatic cancer therapy. *Journal of Nanomedicine Research* **2014**, *1*, <https://doi.org/10.15406/jnmr.2014.01.00004>.
34. Cruje, C.; Chithrani, D.B. Poly ethylene glycol density and length affects nanoparticle uptake by cancer cells. *J. Nanomed.Res.* **2014**, *1*, <https://doi.org/10.15406/jnmr.2014.01.00006>.
35. Malekigorji, M.; Hoskins, C.; Curtis, T.; Varbiro, G. Enhancement of the cytotoxic effect of anticancer agent by cytochrome C functionalised hybrid nanoparticles in hepatocellular cancer cells. *Journal of Nanomedicine Research* **2014**, *1*, <https://doi.org/10.15406/jnmr.2014.01.00010>.
36. Blum, J.L.; Edwards, J.R.; Prozialeck, W.C.; Xiong, J.Q.; Zelikoff, J.T. Effects of maternal exposure to cadmium oxide nanoparticles during pregnancy on maternal and offspring kidney injury markers using a murine model. *Journal of Toxicology and Environmental Health, Part A* **2015**, *78*, 711-724, <https://doi.org/10.1080/15287394.2015.1026622>.
37. Sachet, E.; Shelton, C.T.; Harris, J.S.; Gaddy, B.E.; Irving, D.L.; Curtarolo, S.; Maria, J.P. Dysprosium-doped cadmium oxide as a gateway material for mid-infrared plasmonics. *Nature materials* **2015**, *14*, 414-420, <https://doi.org/10.1038/nmat4203>.
38. Lei, M.; Bi, K.; Zhang, Y.B.; Huang, K.; Fu, X.L.; Wang, X.; Wang, Y.G. Highly selective growth of TiO<sub>2</sub> nanoparticles on one tip of CdS nanowires. *Journal of Alloys and Compounds* **2015**, *646*, 1004-1008, <https://doi.org/10.1016/j.jallcom.2015.06.043>.
39. Yan, L.L.; Li, Y.T.; Hu, C.X.; Li, X.J. Temperature-dependent photo luminescence and mechanism of CdS thin film grown on Si nanoporous pillar array. *Applied Surface Science* **2015**, *349*, 219-223, <https://doi.org/10.1016/j.apsusc.2015.05.001>.
40. Devadoss, I.; Muthukumar, S. Influence of Cu doping on the microstructure, optical properties and photoluminescence features of Cd<sub>0.9</sub>Zn<sub>0.1</sub>S nanoparticles. *Physica E: Low-dimensional Systems and Nanostructures* **2015**, *72*, 111-119, <https://doi.org/10.1016/j.physe.2015.04.022>.
41. Lim, I.; Shinde, D.V.; Patil, S.A.; Ahn, D.Y.; Lee, W.; Shrestha, N.K.; Han, S.H. Interfacial engineering of CdO–CdSe 3D micro architectures with in situ photopolymerized PEDOT for an enhanced photovoltaic performance. *Photochemistry and photobiology* **2015**, *91*, 780-785, <https://doi.org/10.1111/php.12429>.
42. Van, T.K.; Pham, L.Q.; Kim, D.Y.; Zheng, J.Y.; Kim, D.; Pawar, A.U.; Kang, Y.S. Formation of a CdO layer on CdS/ZnO nano rod arrays to enhance their photo electro chemical performance. *Chem Sus Chem* **2014**, *7*, 3505-3512, <https://doi.org/10.1002/cssc.201402365>.

43. Shi, Y.; Chen, Y.; Tian, G.; Wang, L.; Xiao, Y.; Fu, H. Hierarchical Ag/Ag<sub>2</sub>S/CuS Ternary Hetero structure Composite as an Efficient Visible-Light Photocatalyst. *Chem Cat Chem.* **2015**, *7*, 1684-1690, <https://doi.org/10.1002/cctc.201500121>.
44. Chowdhury, P. In silico investigation of phyto constituents from Indian medicinal herb 'Tinospora cordifolia (giloy)' against SARS-CoV-2 (COVID-19) by molecular dynamics approach. *Journal of Biomolecular Structure and Dynamics* **2020**, *39*, 6792-6809, <https://doi.org/10.1080/07391102.2020.1803968>.
45. Sharma, S.; Chaudhary, R.; Rolta, R.; Sharma, N.; Sourirajan, A.; Dev, K.; Kumar, V. Effect of solvent on yield, photochemical and in vitro anti-oxidant potential of Rhododendron arboretum. *Research Journal of Pharmacy and Technology* **2021**, *14*, 311-316, <https://doi.org/10.5958/0974-360X.2021.00057.3>.
46. Kim, N.; Do, J.; Ju, I.G.; Jeon, S.H.; Lee, J.K.; Oh, M.S. Pichrorhiza kurroa prevents memory deficits by inhibiting NLRP3 inflammasome activation and BACE1 expression in 5xFADmice. *Neuro therapeutics* **2020**, *17*, 189-199, <https://doi.org/10.1007/s13311-019-00792-7>.
47. Dhiman, N.; Bhattacharya, A. Nardostachys jatamansi (D.Don) DC.-Challenges and opportunities of harnessing the untapped medicinal plant from the Himalayas. *Journal of ethnopharmacology* **2020**, *246*, <https://doi.org/10.1016/j.jep.2019.112211>.
48. Sharma, V.; Sharma, R.; Gautam, D.S.; Kuca, K.; Nepovimova, E.; Martins, N. Role of Vacha (Acorus calamus Linn.) in neurological and metabolic disorders:evidence from ethnopharmacology, photochemistry, pharmacology and clinical study. *Journal of clinical medicine* **2020**, *9*, <https://doi.org/10.3390/jcm9041176>.
49. Čokeša, V.; Pavlović, B.; Stajić, S.; Poduška, Z.; Jović, Đ. Corylus, L. Its diversity, geographical distribution and morpho-anatomical characteristics with special reference to the systematic classification and phylogenics of Turkishhazel (CoryluscolumnaL.).*Sustainable Forestry:Collection* **2020**, *81-82*, 1-17, <https://doi.org/10.5937/SustFor2081001Q>.
50. Gantait, S.; Mahanta, M.; Bera, S.; Verma, S.K. Advances in biotechnology of Emblica officinalis Gaertn. syn. Phyllanthus emblica L.: a nutraceuticals-richfruit tree with multi faceted ethnomedicinal uses. *3Biotech.* **2021**, *11*, 1-25, <https://doi.org/10.1007/s13205-020-02615-5>.
51. Rajendrachari, S.; Taslimi, P.; Karaoglanli, A.C.; Uzun, O.; Alp, E.; Jayaprakash, G.K. Photo catalytic degradation of Rhodamine B(RhB) dye in waste water and enzymatic inhibition study using cauliflower shaped ZnO nanoparticles synthesized by an ovel One-pot green synthesis method. *Arabian Journal of Chemistry.* **2021**, *14*, <https://doi.org/10.1016/j.arabjc.2021.103180>.
52. Stevenson, A.W.; Milanko, M.; Barnea, Z. An harmonic thermal vibrations and the position parameter in wurtzite structures. I. Cadmium sulphide. *Acta Crystallographica SectionB: Structural Science* **1984**, *40*, 521-530, <https://doi.org/10.1107/S0108768184002639>.
53. Klug, H.P.; Alexander, L.E. *X-ray diffraction procedures:for poly crystalline and amorphous materials.* **1974**; pp.992.
54. Dong, W.; Zhu, C. Optical properties of surface-modified CdO nanoparticles. *Optical Materials* **2003**, *22*, 227-233, [https://doi.org/10.1016/S0925-3467\(02\)00269-0](https://doi.org/10.1016/S0925-3467(02)00269-0).